VOL. 12, NO. 7, APRIL 2017 ISSN 1819-6608
ARPN Journal of Engineering and Applied Sciences
©2006-2017 Asian Research Publishing Network (ARPN). All rights reserved.
www.arpnjournals.com

CFD SIMULATION OF FLOW CONTROL WITH ENERGY PROMOTERS IN S-SHAPED DIFFUSER

Raed A. Jessam, Hussain H. Al-Kayiem and Mohammed Shakir Nasif
Department of Mechanical Engineering, Universiti Teknologi PETRONAS, Bandar Seri Iskandar, Perak, Malaysia
E-Mail: raedabbas2014@yahoo.com

ABSTRACT

This paper presents the computational fluid dynamic (CFD) simulation results for an S-shaped aggressive diffuser. Energy promoters (EPs) were distributed in different locations and configurations along this diffuser to establish its effectiveness in improving flow patterns. The simulated flow field was generated within a normal S-shaped diffuser with a high curvature of 45°/45°, and the total length of this diffuser was reduced by 22%. CFD simulation was performed on both normal and aggressive diffusers, as well as with and without EPs, through ANSYS-FLUENT commercial software. The renormalized group k–ε model was used to simulate turbulence. The simulation results were validated and were consistent with the findings of previous experimental and numerical studies. Results obtained in the current study indicated that the combination of EPs effectively controls flow distortion in S-shaped aggressive diffusers. Performance parameters, such as the coefficients of static pressure recovery and total pressure loss, suggested that the performance of the five pairs of promoters attached to a specific location at the top and bottom surfaces was optimized; pressure recovery was increased by 47% and total loss coefficient was reduced by 56% in comparison with the case of a normal diffuser.

Keywords: computational fluid dynamic (CFD), energy promoters, S-shaped aggressive diffuser, pressure recovery, turbulence models.

INTRODUCTION

Intake is an important component of air breathing engines, and the pressure recovery and efficiency of this component strongly affect engine performance. Among the most commonly applied types of intakes is the S-shaped diffuser, which guides air from around a plane body to the engine inlet [1]. S-shaped diffusers have centerline curvatures and cross-sectional areas that increase along the flow direction. Owing to this centerline curvature, cross-stream pressure gradients build up and increase secondary flows. This phenomenon creates cross-flow velocities within the boundary layer that generate a non-uniform pressure profile at the engine face; this profile is called the Aerodynamic Inlet Plane (AIP). In addition, the adverse streamwise pressure gradient caused by the increasing cross-sectional area can also lead to flow separation. To achieve acceptable performance, an S-shaped diffuser must incur minimal total pressure losses and facilitate almost-uniform flow with small cross-flow velocity components at the AIP [2]. Due to size and weight restrictions, the use of short S-shaped diffusers (aggressive diffusers) is encouraged.

In paper of [3] investigated the effects of an ingested vortex on the flow field of a diffusing S-duct. The ingested vortex at the upstream of the diffusing S-duct reduced the extent of flow-field separation within the baseline duct and promoted the strong cross-flow of the baseline duct with vortex generators. The enhanced cross-flow also strengthened the vortices generated from the vortex generators.

In paper of [4] conducted experiments to study the effect of fences and vortex generators in terms of reducing exit flow distortion and improving total pressure recovery in two-dimensional, rectangular S-duct diffusers with different radius ratios. The fence height and orientation of tapered fin vortex generators varied optimal performance depending on centerline curvature.

A low-profile wishbone type vortex generator [5] used to improve the total pressure distortions and recovery performance of a diffusing S-duct. The configuration that employed the largest vortex generator reduced distortion most effectively, but this configuration did not lead to major total pressure recovery.

Experimentally investigated the flow development within an aggressive interturbine duct with and without the installation of a low-profile vortex generator on the casing [6].Both counter-rotating and corotating configurations were considered, and the latter reduced pressure loss more effectively than the former.

The complex flow pattern in an S-shaped curved diffuser is enhanced further by a number of interrelated geometrical and dynamical parameters, such as Energy Promoters (EPs).The purpose of adding energy promoters EPs is to supply the momentum of flow from higher region where has large momentum to lower region where has small momentum by streamwise vortices generated from EP located just before the separation point, as described by [7]. This process allows the separation point to shift further downstream. This downstream shift lengthens the duration of expanded airflow proportionately, and the flow velocity at the separation point slows as well.

The present work studies flow control in an S-shaped aggressive diffuser with EPs by using ANSYS-FLUENT 14 to simulate the effects of EP on the improvement of flow in such diffusers. Furthermore, this study determines the ideal EP configuration that optimizes diffuser performance.

©2006-2017 Asian Research Publishing Network (ARPN). All rights reserved.

GEOMETRICAL DESCRIPTION AND CFD ANALYSIS OF AN S-SHAPED DIFFUSER

S-shaped diffuser

The complete geometry of the simulated diffuser along with the coordinate system used is shown in Figure-1. It was designed based on area ratio AR of 1.923. The radius of curvature $R_C = 280$ mm, the turning angle $\beta = 45°$, and centerline length $C_L = 440$ mm. The S-shaped aggressive diffuser is similar to the normal S-shaped diffuser in terms of design and AR. The inlets and outlets of the two diffuser types are also similar; however, the total length of the S-shaped aggressive diffuser is 410 mm instead of 526 mm, which is the length of a normal S-shaped diffuser. The turning angle $\beta = 30°$ as indicated in Figure-2.

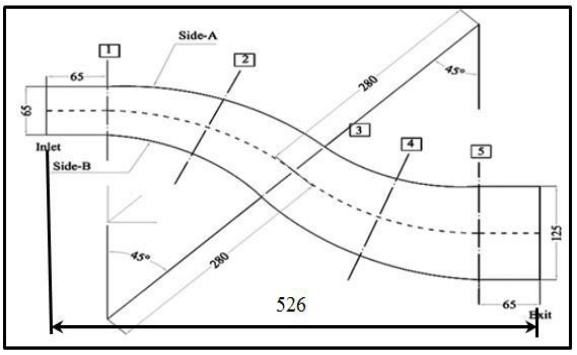

Figure-1. Geometry of S-shaped diffuser (dimensions in mm).

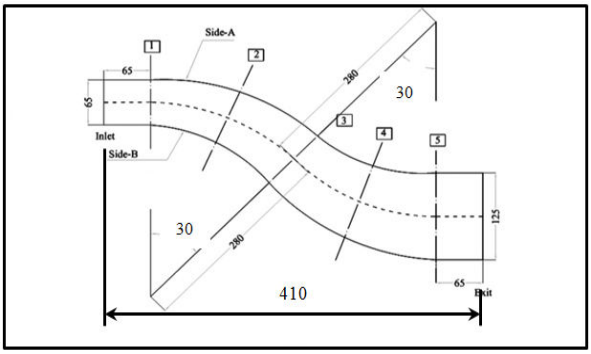

Figure-2. Geometry of S-shaped aggressive diffuse.

The modeled diffuser has a constant area was attached at the inlet of test diffuser with 65x65mm for smooth air inflow and 65x125 mm a constant area tailpipe at the exit of diffuse. The cross-sectional area of the inlet and outlet is 1/8 of the circular cross-sectional areasin the inlets and outlets of both diffuser types, as illustrated in Figure-3.

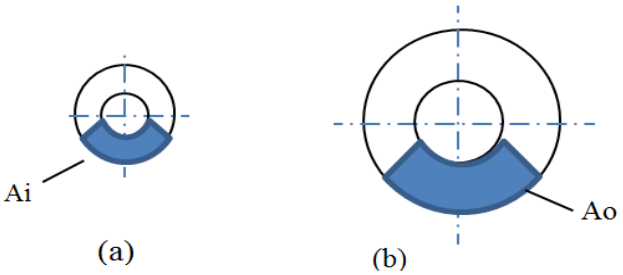

Figure-3. Cross-sectional area of S-shaped diffuser (a) inlet, (b) outlet

Grid generation

The commercial grid generation software GAMBIT is used for preprocessing in this study. The geometry is accurately modeled and is divided into simple parts for easy and quality domain discretization. Hexahedron meshing is conducted to generate the major part of the grid as a structured mesh.

Configurations of energy promoters combinations

EPs were employed to improve the flow pattern at the exit plane of the S-shaped aggressive diffuser and to enhance uniformity. These promoters help delay separation, thereby reducing pressure losses and increasing pressure recovery. Various EP combinations in the diffuser were investigated as follows:

(a) 5 + 5 EPs were attached to top and bottom surfaces and positioned before the inflexion plane at plane 2-2, which was located at $x/C_L = 0.4$

(b) 5 + 5 EPs were attached to top and bottom surfaces and positioned on the inflexion plane at plane 3-3, which was located at$x/C_L = 0.5$

(c) 5 + 5 EPs were attached to top and bottom surfaces and positioned after the inflexion plane at plane 4-4, which was located at$x/C_L = 0.8$

EPs were shaped as half- ellipses with length l = 10 mm, width b = 5 mm, and height h = 3 mm as in Figure-4.

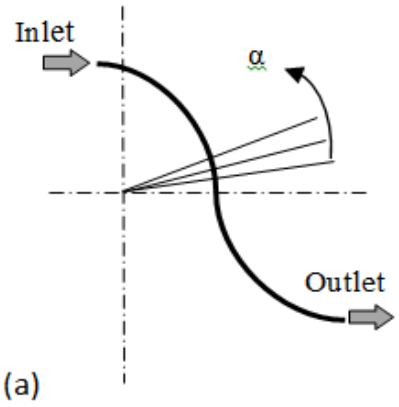

©2006-2017 Asian Research Publishing Network (ARPN). All rights reserved.

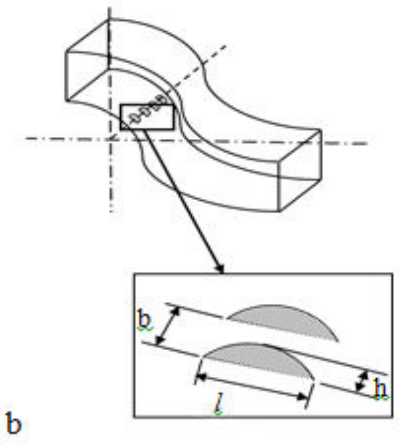

Figure-4. (a) Angular position of energy promoters inside aggressive diffuser, (b) Arrangement and geometry of proposed energy promoters.

The governing equations and boundary conditions

The governing equations for continuity and momentum, Navier-Stokes equations, as well as for steady, turbulent, 3D, and incompressible flows of air are as expressed as follows:

The continuity equation in coordinates (x,y,z)

$$\frac{\partial p}{\partial t}+\frac{\partial}{\partial x}(\rho v_x)+\frac{\partial}{\partial y}\rho vy+\frac{\partial}{\partial z}\rho vz=0 \quad (1)$$

The momentum equations in coordinates (x,y,z)

x-component:

$$\rho\frac{\partial v_x}{\partial t}+v_x\frac{\partial v_x}{\partial x}+v_y\frac{\partial v_x}{\partial y}+v_z\frac{\partial v_x}{\partial z}=-\frac{\partial p}{\partial x}$$
$$-\frac{\partial \tau_{xx}}{\partial x}+\frac{\partial \tau_{yx}}{\partial y}+\frac{\partial \tau_{yx}}{\partial z}+\rho g_x \quad (2)$$

y-component:

$$\rho\frac{\partial v_y}{\partial t}+v_x\frac{\partial v_y}{\partial x}+v_y\frac{\partial v_y}{\partial y}+v_z\frac{\partial v_y}{\partial z}=-\frac{\partial p}{\partial y}$$
$$-\frac{\partial \tau_{xy}}{\partial x}+\frac{\partial \tau_{yy}}{\partial y}+\frac{\partial \tau_{yx}}{\partial z}+\rho g_y \quad (3)$$

z-component:

$$\rho\frac{\partial v_z}{\partial t}+v_x\frac{\partial v_z}{\partial x}+v_y\frac{\partial v_z}{\partial y}+v_z\frac{\partial v_z}{\partial z}=-\frac{\partial p}{\partial z}$$
$$-\frac{\partial \tau_{xy}}{\partial x}+\frac{\partial \tau_{yz}}{\partial y}+\frac{\partial \tau_{zz}}{\partial z}+\rho g_z \quad (4)$$

The simulation was conducted under the following inlet boundary conditions:

Re = Reynolds number of 0.68×10^5 .
Uavi = Average inlet flow velocity of 15.8 m/s
Dh = Hydraulic diameter of the S-shaped diffuser 65 mm.

The inlet conditions above are similar to those of the validated experimental and simulated cases [2]. A constant inlet velocity profile and zero gauge pressure are specified as exit conditions for all simulation cases to facilitate comparative performance evaluation in the CFD simulation of a normal S-shaped diffuser, an S-shaped aggressive diffuser, and an aggressive diffuser with EP. To indicate turbulence quantities, such as turbulence kinetic energy *k* and turbulence dissipation rate ε, the following relations are applied:

$$k=\frac{3}{2}(U_{avi})^2 \quad (5)$$

$$\varepsilon=C_\mu\frac{3}{4}\frac{K^{\frac{3}{2}}}{L}) \quad (6)$$

where:
L = turbulence length scale = $0.07L_c$
L_c = characteristic length,
I = turbulence intensity = $0.16(\mathrm{Re})^{-1/8}$
$C\mu$ = turbulence model constant.

A no-slip boundary condition is specified for the duct walls. Near-wall modeling is performed with enhanced wall treatment method to address the boundary layer formed during grid generation.

PERFORMANCE PARAMETERS

Static pressure recovery coefficient

The static pressure recovery coefficient is represented by the following equation

$$C_{PR}=\frac{P_s-P_{si}}{\frac{1}{2}\rho Uavi^2} \quad (7)$$

Ps = static pressure (N/m^2)
Psi = inlet static pressure (N/m^2)
P = density of air (kg/m^3)

Total pressure loss coefficient

The total pressure loss coefficient is represented by the following equation

$$C_{TL}=\frac{P_{ti}-P_t}{\frac{1}{2}\rho Uavi^2} \quad (8)$$

Pti = inlet total pressure (N/m^2)
Pt = total pressure (N/m^2)

©2006-2017 Asian Research Publishing Network (ARPN). All rights reserved.

Wall static pressure coefficient

The wall static pressure coefficient is represented by the following equation:

$$C_{WPR} = \frac{P_{ws} - P_{wsi}}{\frac{1}{2}\rho U_{avi}^2} \quad (9)$$

Pws = wall static pressure (N/m^2)
$Pwsi$ = wall inlet static pressure (N/m^2)

RESULTS AND DISCUSSIONS

CFD simulation is conducted with ANSYS-FLUENT 14 software. Preliminary investigations are performed in accordance with a turbulence range for a 45°/45° S-shaped diffuser, 30°/30° S-shaped aggressive diffuser, and an aggressive diffuser with EP. The flow field is predicted by the renormalized group (RNG) k–εon the basis of the previous experimental and simulation results obtained by [2].

Static pressure recovery coefficient

The variation in static pressure recovery coefficient C_{PR} along the length of the normal and shaped aggressive diffusers is illustrated in Figure-5, where:

Case (1) - normal S-shaped diffuser.
Case (2) - aggressive diffuser without EP.
Case (3) - aggressive diffuser with EP at plane 2-2.
Case (4) - aggressive diffuser with EP at plane 3-3.
Case (5) - aggressive diffuser with EP at plane 4-4.
Sim – Ref.2simulation results of [2]
Exp – Ref.2experimental results of [2]

The initial phase increases up to plane2-2. However, this growth declines due to flow separation until reattachment occurs at some point after the plane 3-3 $x/C_L = 0.5$. Then, the initial phase increases steadily up to the exit. C_{PR} value is maximized at 0.47 for the 5 + 5 EP pairs attached to the top and bottom surfaces at plane 3-3. As per Figure-6, flow separation starts at $x/C_L = 0.55$for normal diffusers, at $x/C_L = 0.35$for aggressive diffuser case 1, and at $x/C_L = 0.43$for case 4. The present simulation results agree with previous experimental and simulated results.

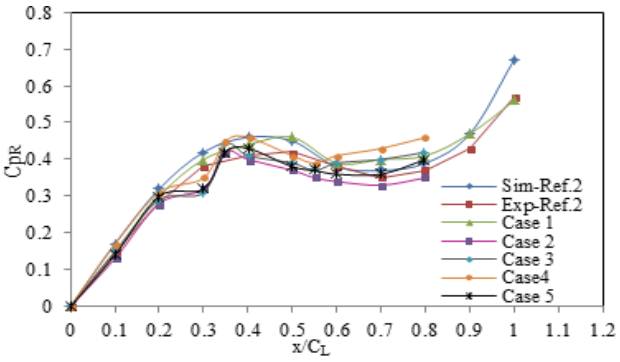

Figure-5. Static pressure recovery coefficient for normal, aggressive diffuser with various EP combinations.

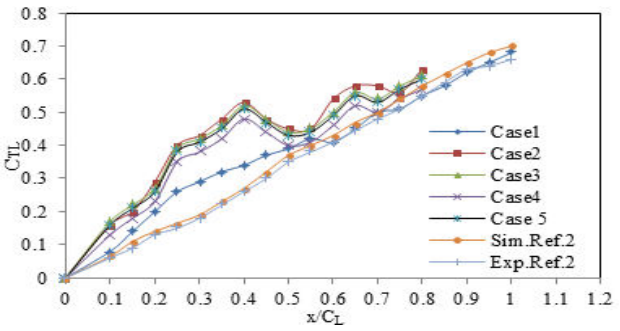

Figure-6. Total pressure loss for normal S-shaped diffuser and aggressive diffuser.

Table-1. Comparison of different cases of S-shaped diffuser with and without Energy Promoters

	Sim. result ref.2	Exp. result ref.2	Case 1	Case 2	Case 3	Case 4	Case 5
CPR	0.671	0.57	0.56	0.35	0.42	0.47	0.4
CTL	0.55	0.58	0.55	0.55	0.61	0.56	0.6

Total pressure loss coefficient

The total pressure loss coefficient C_{TL} along the centerline length of S-shaped diffuser and S-shaped aggressive diffuser presents in Figure-6.The total pressure loss coefficient increases almost linearly along the centerline length for both normal S-shaped diffuser and aggressive S-shaped diffuser. The value of CTL is 0.55 for the normal S-shaped diffuser and maximum CTL for the S-shaped aggressive diffuser is 0.65.This increasing in CTL value is attributed to the early flow separation.

Wall static pressure coefficient

Figure-7 and Figure-8 compare the wall static pressure recovery results along the top and bottom surfaces of the normal and aggressive diffusers with the RNG (k–ε) model, respectively. These results are validated with those of [2]. Flow separation in the normal diffuser starts at $x/C_L = 0.65$, whereas this process begins early at $x/C_L = 0.45$ for S-shaped aggressive diffusers when we reduce the total length of the normal diffuser from 526 mm to 410 mm.

©2006-2017 Asian Research Publishing Network (ARPN). All rights reserved.

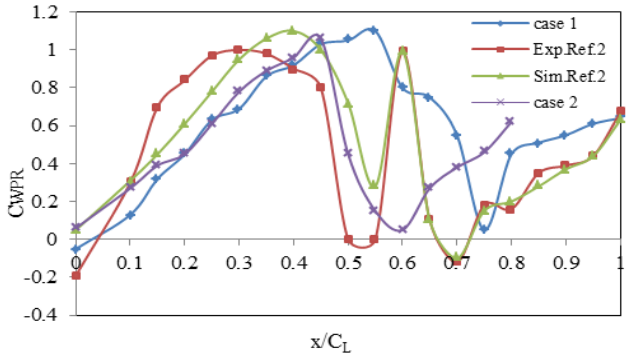

Figure-7. CFD comparison of wall static pressure along top surface between normal and aggressive diffuser.

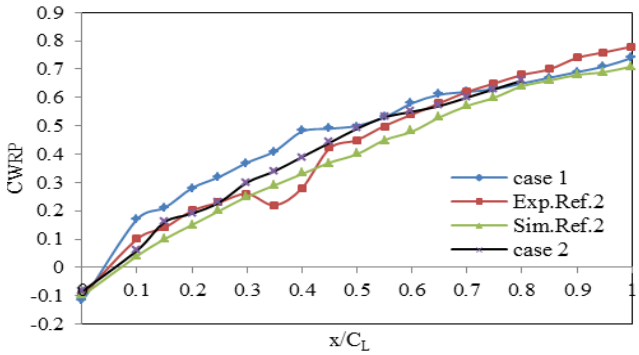

Figure-8. CFD comparison of wall static pressure along bottom surface between normal and aggressive diffuser.

CONCLUSIONS

In this study, a normal S-shaped diffuser and an aggressive S-shaped diffuser are investigated with and without various combinations of EPs through CFD commercial software. The shortening of a normal S-shaped diffuser from 526 mm to 410 mm (aggressive S-shaped diffuser) reduces diffuser efficiency from 0.56 to 0.35 in terms of C_{PR} reduction and increases C_{TL} value from 0.55 to 65. Thus, the uses of EPs limits reverse flow and enhance diffuser efficiency by increasing C_{PR} and reducing C_{TL}. The 5 + 5 pair of EPs that are attached to the top and bottom surfaces in plane 3-3 performed the best among all of the EP combinations tested, with $C_{PR} = 0.47$ and $C_{TL} = 0.56$. The experimental and simulated results of [2] agreed with those of the present study results; thus, the simulation procedure is validated.

REFERENCES

[1] Madadi A., Kermani M. J., and Nili-Ahmadabadi M. 2014. Aerodynamic design of s-shaped diffusers using ball–spine inverse design method. Journal of Engineering for Gas Turbines and Power. 136(12): 122606.

[2] Paul A. R., Ranjan P., Patel V. K., and Jain A. 2013. Comparative studies on flow control in rectangular S-duct diffuser using submerged-vortex generators. Aerospace Science and Technology. 28(1): 332-343.

[3] Reichert B.A. and Wendt B.J. 1996. Improving curved subsonic diffuser with vortex generators. AIAA Journal. 34(1): 65-72.

[4] Sullerey R. K., Mishra S., and Pradeep A. M. 2002. Application of boundary layer fences and vortex generators in improving performance of s-duct diffusers. Journal of fluids engineering. 124(1): 136-142.

[5] Reichert B.A. and WendtB.J.1993. An experimental investigation of s-duct flow control using arrays of low profile vortex generator. AIAA Paper No. 93-0018.

[6] Zhang Y., Hu S., Zhang X. F., Benner M., Mahallati A. and Vlasic E. 2014. Flow control in an aggressive interturbine transition duct using low profile vortex generators. Journal of Engineering for Gas Turbines and Power. 136(11): 112604.

[7] Abdellatif O. E. 2006. Experimental study of turbulent flow characteristics inside a rectangular s-shaped diffusing duct. AIAA Aerospace Sciences Meeting and Exhibit, AIAA-2006-1501, Reno, Nevada.